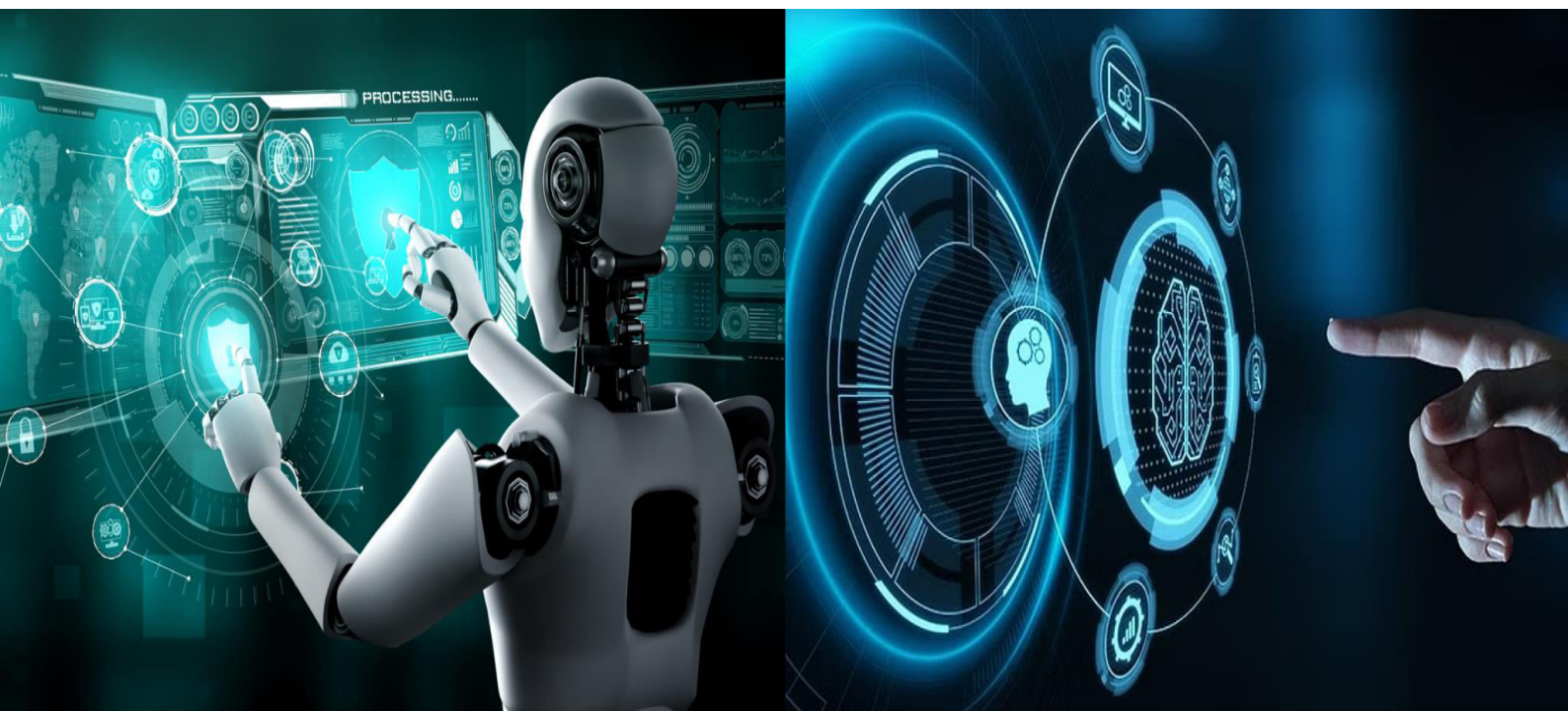


# International Journal of Innovative Research in Computer and Communication Engineering

(A Monthly, Peer Reviewed, Refereed, Scholarly Indexed, Open Access Journal)





# A Broadband Met material Absorber for Applications at Mid Infrared Frequency

T Varsha Sri<sup>1</sup>, S Srivallika<sup>1</sup>, M P Srinivasa Rao<sup>2</sup>

U.G. Student, Department of Electronics and Communication Engineering, GMR Institute of Technology, Rajam, Andhra Pradesh, India<sup>1</sup>

Professor, Department of Basic Sciences and Humanities, GMR Institute of Technology, Rajam, Andhra Pradesh, India<sup>2</sup>

**ABSTRACT:** The infrared region holds a crucial role within the electromagnetic spectrum. Conventional infrared devices primarily rely on the intrinsic characteristics of natural materials to manipulate electromagnetic waves, however, their limited control capabilities often fall short of fulfilling current technological demands. In this study, we proposed a metal–dielectric–metal metamaterial configuration. The device has been optimized with structural dimensions at which its absorption properties are analyzed. Numerical results demonstrate that the absorber has broad absorption peak, which is result from magnetic polariton modes generated at different resonant wavelengths. The structure achieves an absorption exceeding 99.8% over a spectral width of 1000 nm, across the mid infrared band (7.33  $\mu\text{m}$  - 8.33  $\mu\text{m}$ ). Featuring a simple structure, ease of fabrication, and the use of readily available materials, the proposed metamaterial offers broad absorption bandwidth. Such structure will assist in designing absorbing element for infrared spectroscopy and imaging.

**KEYWORDS:** Metamaterial; Absorption; Broadband; Mid infrared region

## I. INTRODUCTION

Metamaterials, composed of artificially engineered subwavelength structures, exhibit electromagnetic behaviors that are rarely or never observed in nature. These synthetic composites can be tailored to display extraordinary effects such as a negative refractive index [1], superlenses [2], optical cloaking [3], and electromagnetically induced transparency [4]. A particularly impactful subset of this field, metamaterial perfect absorbers [5-7], has attracted significant interest due to their potential for achieving near-total absorption of electromagnetic radiation. Over the past decade, researchers have investigated how material composition and geometric configurations influence absorption capabilities. In 2008, Landy and collaborators [8] introduced a metamaterial with almost 100% absorption in the microwave spectrum, marking a pivotal moment for metamaterial perfect absorbers. Later in 2014, Ma's team advanced this work by demonstrating a dual-band absorber in the mid-infrared region, reaching absorption rates of 90% and 88% at 4.17  $\mu\text{m}$  and 4.86  $\mu\text{m}$ , respectively [9]. As demands for broader functional frequencies have intensified, the design focus has shifted toward absorbers capable of operating across increasingly wide spectral bands from microwave and terahertz to infrared and even visible light [10-11].

Metamaterial absorbers are generally categorized into narrowband and broadband types, depending on the width of their effective absorption spectrum. Narrowband absorbers excel at capturing energy within a tightly confined range, but such specialization limits their versatility, especially in real-world applications where broader absorption is preferred. This constraint arises primarily from the resonant nature of their underlying structures, which inherently restricts the spectral range. Consequently, researchers have prioritized broadband designs. Several strategies have been pursued to enhance absorption bandwidth, such as coupling multiple resonant units or refining specific features like square ring resonators with narrow gaps. Although these methods can extend bandwidth to some extent, they often introduce manufacturing complexity, high costs, and scaling issues, which hamper their integration into large-scale or commercial systems.

In parallel, the increasing global focus on renewable energy and environmental sensing has intensified interest in harnessing sunlight, particularly its infrared component. The solar spectrum includes ultraviolet, visible, and infrared radiation [12]. While atmospheric gases like water vapor, CO<sub>2</sub>, and ozone attenuate much of the infrared light, specific



## International Journal of Innovative Research in Computer and Communication Engineering (IJIRCCE)

(A Monthly, Peer Reviewed, Refereed, Scholarly Indexed, Open Access Journal)

wavelength bands can still traverse the atmosphere effectively. Infrared radiation, especially in the mid- and long-wave regions, has substantial utility across applications like biomedical diagnostics, gas sensing, military surveillance, and night vision. Despite these prospects, there has been comparatively limited exploration into mid to long wave infrared metamaterial absorbers, underscoring the need for innovation in this spectral range. Addressing this gap, we developed an absorber structure based on metal-dielectric-metal. By leveraging impedance matching and the resonance properties of metal-dielectric-metal (MDM) systems, our design achieves ultra-wideband performance.

We propose a new structure to realize broadband absorption in the mid infrared wavelength region. This design takes into account the simple structure, easy fabrication, and lower cost in practical applications. This metal-dielectric-metal metamaterial absorber consists of gold metal and SiC dielectric layer. The upper meta layer is in two L shapes symmetrically placed with certain distance apart. It is shown that the absorber has broad absorption band from 7.2  $\mu\text{m}$  to 8.3  $\mu\text{m}$  with an average absorptivity of more than 99%. The present study of metamaterial absorber has important application prospects in solar cells, satellite radio thermographs, photodetectors and spectrum imaging.

### II. STRUCTURAL DESIGN AND SIMULATION

The design schematic for the proposed double L symmetrically placed metamaterial absorber is depicted in Fig. 1(a) and Fig. 1(b). In this structure, gold is used for both the L shaped resonator patch and the underlying metallic layer. The dielectric behavior of gold is described using the Drude model, where the dielectric function follows

$$\varepsilon = 1 - \frac{\omega_p^2}{\omega(\omega + i\omega_c)}$$

The plasma frequency  $\omega_p = 1.2 \times 10^{16}$  rad/s and the collision frequency  $\omega_c = 10.5 \times 10^{13}$  rad/s are considered within the wavelength range of 5  $\mu\text{m}$  to 10  $\mu\text{m}$  [13]. As the dielectric spacer, silicon carbide (SiC) is considered, having a dielectric constant of 10.8 and a loss tangent of 0.003. The SiC layer thickness is  $t_d = 0.42$   $\mu\text{m}$ , while the gold film thickness is  $t_m = 0.1$   $\mu\text{m}$ . The unit cell is arranged periodically with a lattice period  $P = 2.6$   $\mu\text{m}$  in both x and y directions and the vertical distance between two L-shaped patches is  $d_1 = 0.4$   $\mu\text{m}$ . The geometrical parameters of the L-shaped patch are defined by its width  $W$  and length  $L$  are 0.4  $\mu\text{m}$  and 0.8  $\mu\text{m}$  respectively. The transmission and reflection coefficients are computed using a finite element method tool, COMSOL Multiphysics. The simulation assumes a transverse electric (TE) wave incident in the x-z plane, with an incident angle  $\theta$  relative to the z-axis (the azimuthal angle  $\varphi = 0^\circ$ , which is the angle between the projection of incident light on x-y plane and x-direction), as illustrated in Fig. 1(a). Periodic boundary conditions are applied along both the x and y axes.

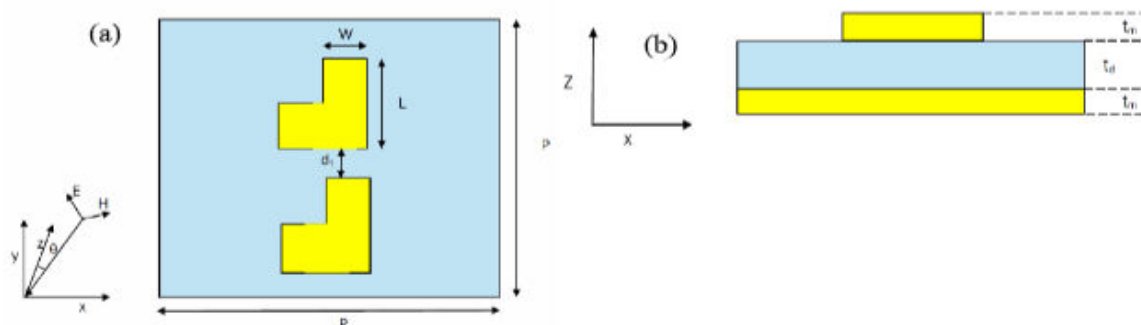


Fig. 1. (a) Top view and (b) cross-sectional view of a unit cell of the double L symmetrically placed metamaterial absorber.

### III. RESULTS AND DISCUSSION

As the gold film's thickness is much larger than the material's infrared skin depth, the absorption ( $A$ ) can be determined using the formula  $A = 1 - |S_{11}|^2$  where  $|S_{11}|$  denotes the reflection coefficient. The simulated absorption curve for the double L symmetrically placed absorber within the wavelength range of 5  $\mu\text{m}$  to 10  $\mu\text{m}$  is presented in Fig. 2 for an incidence angle of  $\theta = 45^\circ$  and azimuthal angle  $\varphi = 0^\circ$  for TE mode. A remarkable observation from the figure that absorption 99.8 % is observed from 7.33  $\mu\text{m}$  to 8.33  $\mu\text{m}$ .



## International Journal of Innovative Research in Computer and Communication Engineering (IJIRCCCE)

(A Monthly, Peer Reviewed, Refereed, Scholarly Indexed, Open Access Journal)

The absorption spectra of the double L symmetrically placed structure for an incidence angle of  $\theta = 45^\circ$  and azimuthal angle  $\varphi = 0^\circ$  for TE mode at different thickness of SiC are shown in Fig.3. For TE mode, two absorption peaks are observed at  $5.86 \mu\text{m}$  (99.98%) and  $7.54 \mu\text{m}$  (99.96%) for SiC thickness  $0.27 \mu\text{m}$ . The absorption gradually increases when the thickness of the dielectric layer increases from  $0.27 \mu\text{m}$  to  $0.42 \mu\text{m}$  and shows a spreading of maximum absorptivity increase. Therefore, changing thickness of the dielectric layer has a large impact on the magnitude of absorption and range of wavelengths, and optimization leads in the wide range absorption reaching its maximum at  $t_d = 0.42 \mu\text{m}$ .

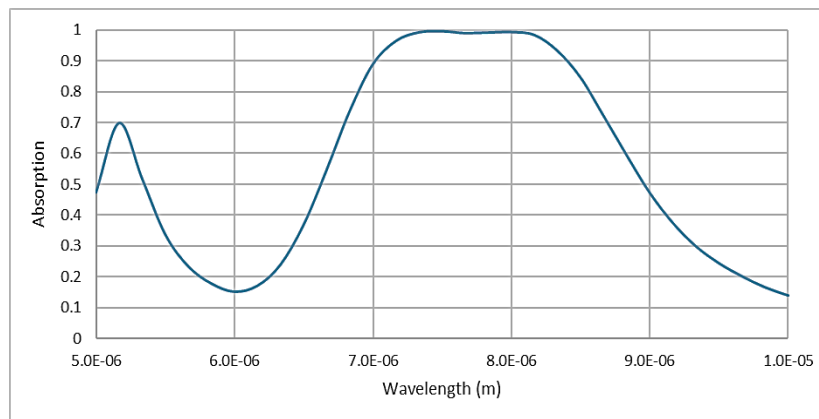


Fig. 2. The absorption spectrum of the double L symmetrically placed metamaterial absorber under the incident angle of  $\theta = 45^\circ$  and  $\varphi = 0^\circ$  for TE mode.

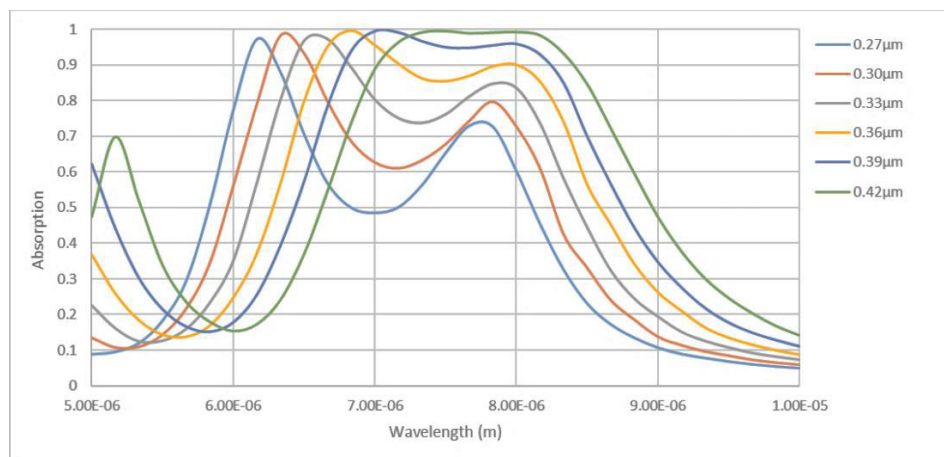


Fig. 3. Absorption spectra of double L symmetrically placed metamaterial with different dielectric thickness ( $t_d$ ) for TE under the incident angle of  $\theta = 45^\circ$  and  $\varphi = 0^\circ$ .

To clarify the mechanism behind the observed absorptions, we studied the electric field distribution across the metamaterial. Fig. 4 and Fig. 5 display the z-component of the electric field distributions at resonant wavelengths  $\lambda_1 = 7.33 \mu\text{m}$  and  $\lambda_2 = 8.33 \mu\text{m}$ . As shown in Fig. 4(a), at  $\lambda_1$ , the electric field is primarily concentrated at the bottom corners (the horizontal x-axis) of the L-shaped elements, while the top vertical (y-axis) arms exhibit weaker field intensities. Simultaneously, Fig. 4(b) illustrates that the electric field on the bottom metallic layer at this wavelength is out of phase with the top layer, suggesting the formation of current loops within the SiC dielectric spacer. This pattern confirms the excitation of magnetic polaritons in each L-shaped patch, resulting in strong magnetic resonances



## International Journal of Innovative Research in Computer and Communication Engineering (IJIRCCCE)

(A Monthly, Peer Reviewed, Refereed, Scholarly Indexed, Open Access Journal)

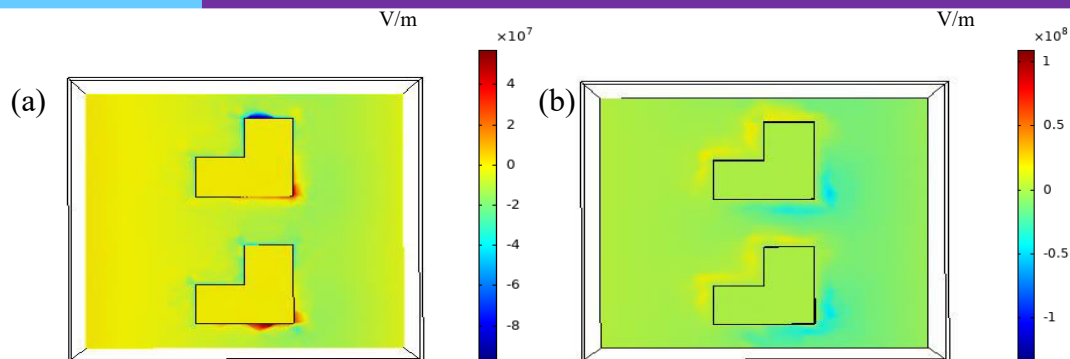


Fig. 4. The z component of electric field distribution at resonant wavelength  $\lambda_1 = 7.33 \mu\text{m}$  on (a) double L symmetrically placed patches and (b) bottom metal layer in TE wave incidence under the incident angle of  $\theta = 45^\circ$  and  $\varphi = 0^\circ$ .

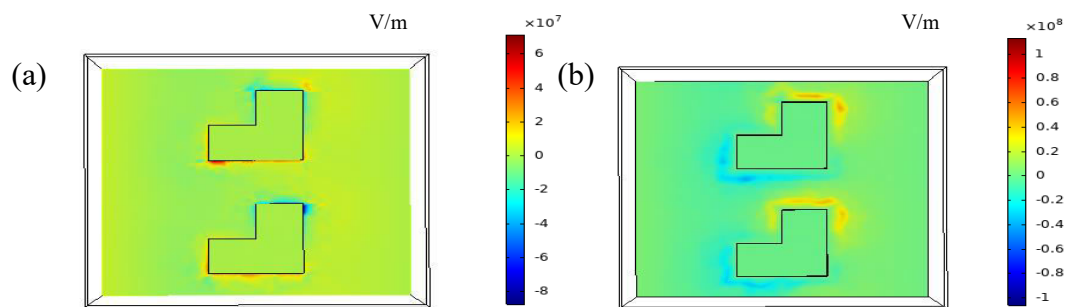


Fig. 5. The z component of electric field distribution at resonant wavelength  $\lambda_2 = 8.33 \mu\text{m}$  on (a) double L symmetrically placed patches and (b) bottom metal layer in TE wave incidence under the incident angle of  $\theta = 45^\circ$  and  $\varphi = 0^\circ$ .

At the resonant wavelength  $\lambda_2 = 8.33 \mu\text{m}$ , Fig. 5(a) shows that the electric field intensifies around the lower corners of the L-shaped patches, while the field is notably weaker at top of the vertical strip. Fig. 5(b) indicates that the electric field distribution at the bottom metal layer remains phase-opposed relative to the patches, once again forming two current loops at the corners of the SiC spacer. This indicates that different magnetic polariton modes are excited at different wavelengths, which generate broad band absorption.

### IV. CONCLUSION

We have carried out numerical simulations of a double L symmetrically placed metamaterial infrared absorber. The absorber is composed of a SiC dielectric spacer, flanked by double L-shaped gold resonators and a continuous gold backing. Broad band absorption is achieved for dielectric thickness of  $t_d=0.42 \mu\text{m}$ . Moreover, variations in the dielectric thickness have been studied to understand their impact on the absorption behavior. Based on the z-component electric field distributions, it is evident that the broad band absorption results from distinct magnetic polariton resonances formed at different wavelengths. This broad band metamaterial absorber holds promising potential for applications in thermal sensing and infrared imaging technologies.

### REFERENCES

1. R. A. Shelby, D. R. Smith, and S. Schultz, 'Experimental verification of a negative index of refraction', Science, Vol. 292(5514), pp.77-79, 2001.
2. D. R. Smith, J. B. Pendry, and M. C. K. Wiltshire, 'Metamaterials and negative refractive index', Science, Vol.305(5685), pp. 788-792, 2004.



## International Journal of Innovative Research in Computer and Communication Engineering (IJIRCCE)

(A Monthly, Peer Reviewed, Refereed, Scholarly Indexed, Open Access Journal)

3. W. Cai, K. U. Chettiar, A. V. Kildishev, and V. M. Shalaev, 'Optical cloaking with metamaterials', *Nat. Photonics*, Vol.1(4), pp. 224-227, 2007.
4. Sen Hu, Dan Liu, Helin Yang, 'Manipulation of electromagnetically induced transparency in all-dielectric metamaterials: From on-off to double transparent windows', *Optik*, Vol. 223, pp. 165637, 2020.
5. Boyi Chen, Shujun Yu, Wenqiang Lu, Zhiqiang Hao, Zao Yi, Shubo Cheng, Can Ma, Chaojun Tang, Pinghui Wu, Sohail Ahmad, 'Mid-infrared bimodal wide metamaterial absorber based on double-layer silicon nitride structure', *Materials Research Bulletin*, Vo. 174, 112751, 2024.
6. Musa, A., Alam, T., Islam, M.T., Hakim, M.L., Rmili, H., Alshammari, A.S., Islam, M.S., Soliman, M.S., 'Broadband Plasmonic Metamaterial Optical Absorber for the Visible to Near-Infrared Region', *Nanomaterials*, Vol.13, pp.626, 2023.
7. Li F, Du J, Wang S, Yu R, Wang X, Zhang T, Chi Z, Wang B and Li N, 'Ultra-broadband infrared metamaterial absorber based on MDMDM structure for optical sensing', *Front. Astron. Space Sci.*, Vol.10, 2024.
8. Landy, N. I., Sajuyigbe, S., Mock, J. J, Smith, D. R., and Padilla, W. J, 'Perfect Metamaterial Absorber', *Phys. Rev. Lett.* Vol.100, pp.207402, 2008.
9. W. Ma, Y. Wen and X. Yu, 'Theoretical and Experimental Demonstrations of a Dual-Band Metamaterial Absorber at Mid-Infrared', *IEEE Photonics Technology Letters*, vol. 26, pp. 1940-1943, 2014.
10. Raeen, M.S., Nella, A., Aldhaheri, R.W, 'A high-performance ultra-compact plasmonic metamaterial structure for optical THz absorption', *Sci Rep*, Vol.14, 27203, 2024.
11. Zheng, H.; Pham, T.S.; Chen, L.; Lee, Y, 'Metamaterial Perfect Absorbers for Controlling Bandwidth: Single-Peak/ Multiple-Peaks/Tailored- Band/Broadband', *Crystals* Vol.14 (19), 2024.
12. M.J.; Rahman, M.H.; Faruque, M.R.I., 'An Innovative Polarisation-Insensitive Perfect Metamaterial Absorber with an Octagonal-Shaped Resonator for Energy Harvesting at Visible Spectra', *Nanomaterials*, Vol.13(1882), 2023.
13. W G. Yeo, N. K. Nahar, and K. Sertel, 'Far-IR multiband dual-polarization perfect absorber for wide incident angles', *Microw. Opt. Technol. Lett.* Vol. 55(3), pp. 632–636, 2013.



INTERNATIONAL  
STANDARD  
SERIAL  
NUMBER  
INDIA



SJIF Scientific Journal Impact Factor



# INTERNATIONAL JOURNAL OF INNOVATIVE RESEARCH

IN COMPUTER & COMMUNICATION ENGINEERING



9940 572 462



6381 907 438



ijircce@gmail.com



[www.ijircce.com](http://www.ijircce.com)

Scan to save the contact details